Chapter 4

Decentralized Scheduling of Multi-Microgrid

4.1 Introduction

The decentralized economic scheduling of Multi-Microgrid (MMG) is an important aspect in the operational planning of Microgrids (MGs). The previous chapter addresses the Dantzig-Wolfe Decomposition Method (DWDM) based decentralized approach to energy management. This approach is carried forward in this chapter for multi-agents based decentralized economic scheduling of MMG. This chapter proposes a novel decentralized Energy Management System (EMS) for networked MMG to optimize the energy resources owned by Microgrid Operator (MGO) and energy resources owned by prosumers. The process of optimization also ensures minimum mandatory information sharing among MGOs and prosumers. The cooperative scheduling to maximize economic benefit among MGs is achieved via price signals encouraging MGs to share power among themselves for economic benefits. The proposed power exchange framework, unlike present approaches in literature, does not require any coupling constraint between MGOs; thereby eliminating the mandatory need for information exchange between MGOs, and also eliminating need of joint scheduling of all MGs for cooperative operations. Each MGO is only required to submit its power exchange request to an external agent called MGs' Aggregator (MGA). The MGA communicates a new price signal for each MGO, based on the contributions of each MGO to the energy pool. The Shapley Value Method (SVM) is used for generating fair price signals for each of the contributing MGO. All MGOs can reschedule their assets

independently based on the price signal.

Additionally, the Parking Lots (PLs) and Distributed Battery Energy Storage Systems (D-BESSs) are considered as profit-based entities. An MGO generates a time-variable tariff based on energy trading status so that the PL operator and D-BESS aggregator participate with flexibility in the MG's energy management. The Stochastic Dantzig-Wolfe Decomposition (SDWD) is used to solve the resulting optimization problem in a decentralized manner. The uncertainties related to load demand and renewable energy sources (RESs) are captured using scenario-based methods, whereas the uncertainty associated with plug-in hybrid electric vehicles (PHEVs) is modeled using copula theory-based estimation.The above said contributions of this chapter are achieved in the following manner.

- A SVM based framework is developed for the cooperative operation of MGs to reduce the operating cost. The SVM is used to fairly allocate profit/cost at the MGA level on hourly basis, which is used to determine the updated electricity tariff for individual MGO.
- A Stochastic Dantzig-Wolfe Decomposition (SDWD) approach is applied for decentralized scheduling of MGs and their prosumers, i.e., PLs and D-BESSs.
- MGO's trading status-based time-variable tariffs are used to emphasize the flexibility and contribution of PLs and D-BESSs in MG's energy management.

4.2 System architecture

In this chapter, the energy management of MMG is considered as optimization of energy cost as an objective. Each MG consists of the following (i) Micro Turbines (MTs), (ii) RESs (Wind Turbines (WTs) and Photovoltaics (PVs)) [127], (iii) prosumers (PLs and D-BESSs) and (iv) consumer loads. The schematic diagram of microgrid on bus is given in Figure 4.1. The different components of the framework and their communication links are illustrated in Figure 4.2. All the MGs can trade power among themselves or with Distribution Utility (DU). The PL operator and D-BESS aggregator are self-governed entities, but they have to follow some constraints or agreements like the maximum limit of power demand etc. MGO offers electricity tariff to PL operator and D-BESS aggregator.

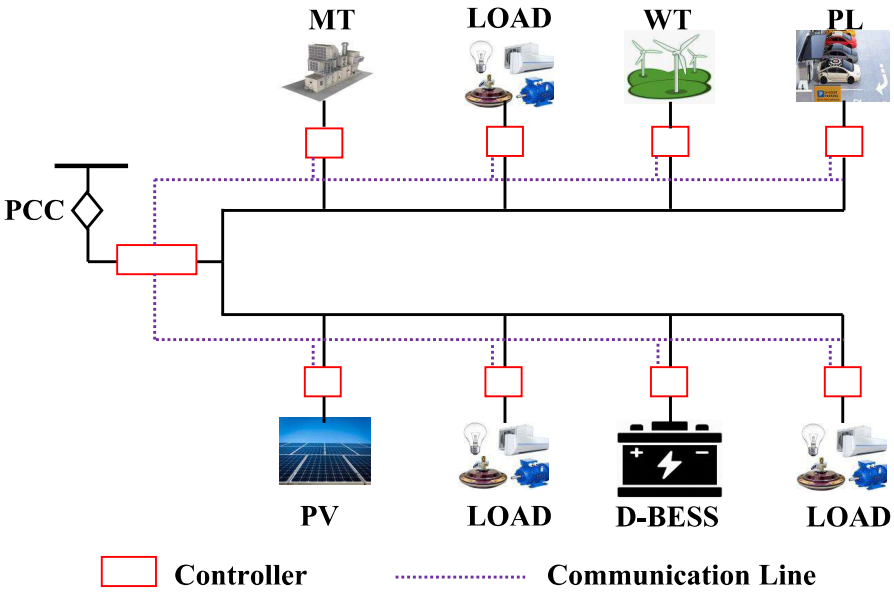

Figure 4.1: Schematic diagram of microgrid

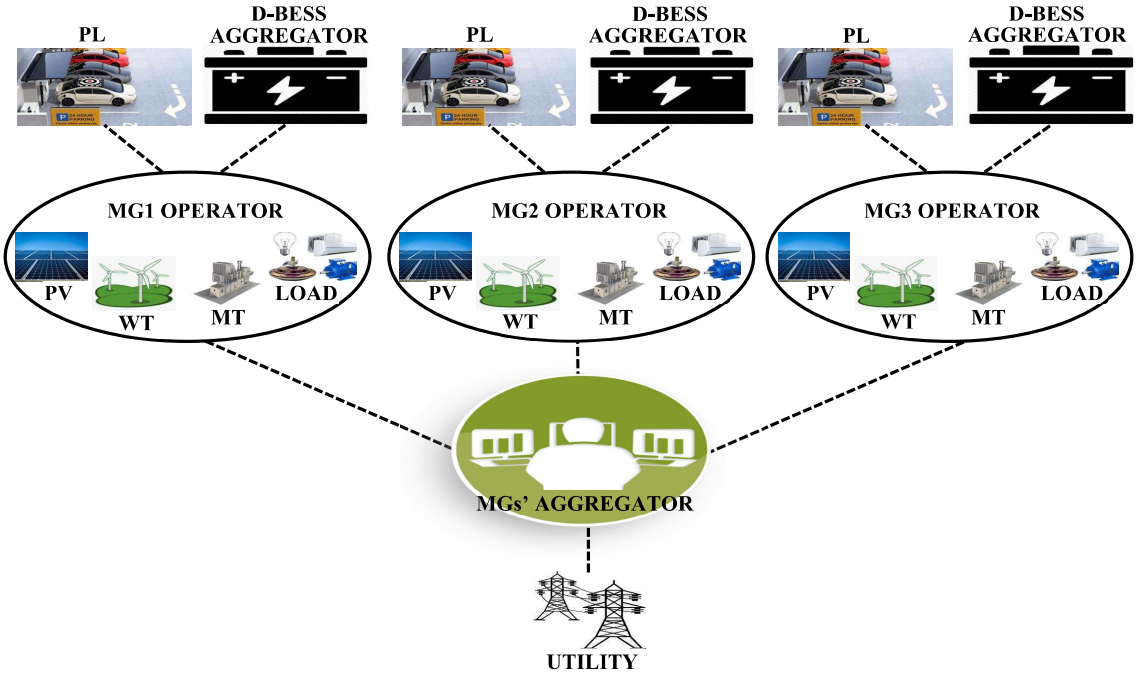

Figure 4.2: Conceptual diagram of MMG energy management framework

In response to the tariff, PL operator and D-BESS aggregator submit their demands to MGO. Each MGO receives electricity tariff from MGA and independently schedules its energy resources to satisfy the demand from PLs, D-BESSs and conventional users. After scheduling its own energy resources, MGO sends a power exchange request to MGA. On the basis of each MG participation, MGA allocates power transfer between MGs or between MG and DU, and updates electricity tariffs for each MG.

4.2.1 Stochastic Model of Parking Lot

The power exchange capability, i.e., PL to Grid (PL2G) and Grid to PL (G2PL), of PLs depends on their customers' driving habits and the type of their vehicles. Arrival time, departure time, and daily driven miles are driving habit related parameters, while the battery capacities and rated charging/discharging power depend on the type of vehicles. In this work, the National Household Travel Survey (NHTS) 2017 database [**?**] is used to model the stochastic driving pattern. The NHTS 2017 database contains 129,112 household surveys. We consider the first trip end time as the arrival time of PHEV in PLs and the next trip start time as the departure time of PHEV from PLs. According to NHTS 2017 database, the arrival time and departure time for PHEVs can be described by Generalized Extreme Value (GEV) distribution whereas, the miles driven by PHEVs can be described by log-normal distribution. The arrival time, departure time and miles driven by PHEVs are described respectively as $GEV(0.0693, 8.528, 2.479)$, $GEV(-0.491, 15.551, 4.025)$ and $Lognormal(3.142, 1.0271)$. The Probability Density Function (PDF) of $GEV(\kappa, \upsilon, \varsigma)$ distribution of arrival and departure time of PHEVs can be described as

$$PDF = \begin{cases} \left(\frac{1}{\varsigma}\right)\left(1+\kappa\frac{(t-\upsilon)}{\varsigma}\right)^{-\frac{(\kappa+1)}{\kappa}} e^{-\left(1+\kappa\frac{(t-\upsilon)}{\varsigma}\right)^{-\frac{1}{\kappa}}}, & \kappa \neq 0 \\ \left(\frac{1}{\varsigma}\right) e^{-\left(\frac{(t-\upsilon)}{\varsigma}+e^{-\frac{(t-\upsilon)}{\varsigma}}\right)}, & \kappa = 0. \end{cases}$$

Here, κ, υ, and ς are the shape, location, and scale parameters, respectively.
Similarly, the PDF of $Lognormal(\bar{\upsilon}, \bar{\varsigma}^2)$ distribution of daily miles driven by PHEVs can be expressed as

$$PDF = \frac{1}{\Gamma\bar{\varsigma}\sqrt{2\pi}} e^{\left(-\frac{(ln\Gamma-\bar{\upsilon})^2}{2\bar{\varsigma}^2}\right)}.$$

Here, $\bar{\varsigma}$ and $\bar{\upsilon}$ are standard deviation and mean of $ln\Gamma$, respectively. Γ represents the miles driven by PHEVs.

Histograms of arrival time, departure time and driven miles are shown in Figure 4.3. As depicted in Figure 4.3(a), the arrival time of about 70% PHEVs is between 7:00-12:00 hours, while the departure time of about 70% PHEVs is between 15:00-21:00 hours. Each bar in Figure 4.3(b) represents the percentage of PHEVs for a particular mileage range. Approximately 70% PHEVs drive less than 40 miles per day.

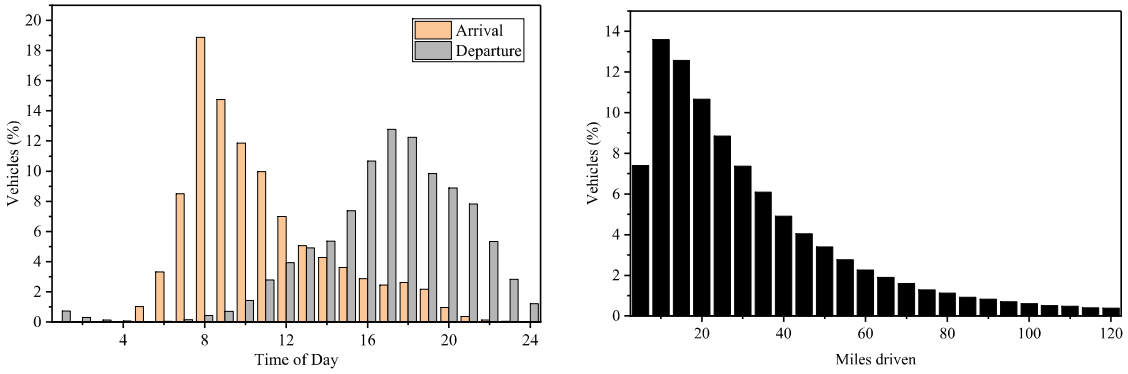

(a) (b)

Figure 4.3: Histogram of (a) Arrival and departure time, (b) Daily miles driven by PHEVs

Based on NHTS 2017 database, the rank correlation between arrival time, departure time, and daily driven miles are shown in Equation (4.1), verifying the monotonic dependency of these three parameters.

$$\tau = \begin{array}{c} \begin{matrix} \text{Arrival} & \text{Departure} & \text{Miles} \end{matrix} \\ \begin{bmatrix} 1 & 0.0761 & -0.1029 \\ 0.0761 & 1 & 0.1334 \\ -0.1029 & 0.1334 & 1 \end{bmatrix} \end{array} \begin{matrix} \\ \text{Arrival} \\ \text{Departure} \\ \text{Miles} \end{matrix} \tag{4.1}$$

A copula function can be employed to find the joint distribution function of these three statistically dependent parameters with different marginal distributions. A copula function joins the uni-variate marginal distribution of random variables to form the multivariate distribution function. For modeling the driving behavior of PHEVs' users, the Gaussian copula is used in this work. The detailed procedure for simulating dependent random parameters using copula can be found in [128]. It is to be noted that these three parameters are used to estimate the energy exchange pattern of PLs for the upcoming day. The real-time arrival/departure time of PHEVs may differ, but the copula theory-based

simulated parameters can forecast the cumulative demand pattern of all PHEVs in PLs. Based on simulated miles driven data, the initial battery status of PHEV, $SoC^{ev}_{t_{arri}}$ can be calculated as

$$SoC^{ev}_{t_{arri}} = \begin{cases} \left(1 - \frac{\Gamma\Upsilon}{\Gamma_{aer}}\right)100, & \Gamma\Upsilon \leq \Gamma_{aer} \\ 0, & \Gamma\Upsilon \geq \Gamma_{aer}. \end{cases}$$

Here, Γ, Υ, and Γ_{aer} represent the miles driven by PHEV, the fraction of miles driven in electric mode and the all-electric range of PHEV, respectively.

4.3 Problem formulation for energy cost minimization

The goal of this study is to minimize the operating cost of MG (f_{MG}), PLs (f_{PL}), and D-BESSs (f_{D-BESS}). The energy cost minimization function (F) can be defined as

$$min\ F = f_{MG} + f_{PL} + f_{D-BESS}. \tag{4.2}$$

All the three components of the energy cost function, F, are subjected to some distinctive and coupling constraints. The uncertainties related to RESs power and consumer loads are simulated through Monte-Carlo Simulation (MCS) based scenarios. MCS is used to generate a large number of samples of RESs generation and consumer loads. It is a very time-consuming process to simulate the scheduling algorithm with such a large number of samples. The scenario reduction algorithm [129] is used to reduce the number of scenarios generated in MCS to an appropriate number to reduce computational complexity. The components f_{PL}, f_{D-BESS} and f_{MG} with their constraints are described in the following section.

4.3.1 Parking lots and distributed battery energy storage cost function

The purpose of the PL operator is to reduce the operating cost of the PL under the tariff structure provided by the MGO with the satisfaction of the owners of the PHEVs. It is assumed that the PLs are equipped with both PL2G and G2PL facility. The operating cost of PLs can be defined as the difference between the cost of energy purchase in G2PL

mode and the income from energy feed-back to MG in PL2G mode. Thus, f_{PL} can be expressed as

$$f_{PL} = \sum_{s=1}^{N_s} \pi_s \sum_{t=1}^{T} (P_{t,s}^{in,PL} \rho_t^c - P_{t,s}^{out,PL} \rho_t^d). \tag{4.3}$$

Here, π_s is the probability of scenario s. The G2PL power, $P_{t,s}^{in,PL}$, and PL2G power, $P_{t,s}^{out,PL}$, can be defined as

$$P_{t,s}^{in,PL} = max\left(0, \sum_{ev=1}^{N_{ev}} (P_{t,s}^{c,ev} - P_{t,s}^{d,ev})\right),$$

$$P_{t,s}^{out,PL} = max\left(0, \sum_{ev=1}^{N_{ev}} (P_{t,s}^{d,ev} - P_{t,s}^{c,ev})\right).$$

The D-BESS aggregator stores energy during a low tariff period and feeds back to MG during a high tariff period. The objective of the D-BESS aggregator is to maximize their profit ($-f_{D-BESS}$). The component related to D-BESSs, f_{D-BESS}, in the cost function, F, can be described as

$$f_{D-BESS} = \sum_{s=1}^{N_s} \pi_s \sum_{t=1}^{T} \sum_{b=1}^{N_{bess}} (P_{t,s}^{c,b} \rho_t^c - P_{t,s}^{d,b} \rho_t^d). \tag{4.4}$$

Here, $P_{t,s}^{c,b}$ and $P_{t,s}^{d,b}$ denote the charging and discharging power of D-BESS, respectively.

Both PHEVs and D-BESSs are subjected to following constraints.

$$P_{t,s}^{c} \leq \nu_{t,s} P^{cmax}, \tag{4.5}$$

$$P_{t,s}^{d} \leq (1 - \nu_{t,s}) P^{dmax}, \tag{4.6}$$

$$SoC_{t,s} = SoC_{t-1,s} + \frac{100}{BC}\left(\eta_c P_{t,s}^{c} - \frac{P_{t,s}^{d}}{\eta_d}\right), \tag{4.7}$$

$$SoC^{min} \leq SoC_{t,s} \leq SoC^{max}, \tag{4.8}$$

$$SoC_{t_{depa},s}^{ev} = min\left[SoC^{max}, \left(SoC_{t_{arri}}^{ev} + \frac{100 \times \eta_c P_{max}^{c,ev} \Delta T}{BC^{ev}}\right)\right], \tag{4.9}$$

$$\sum_{t=1}^{T} \eta_c P_{t,s}^{c,b} = \sum_{t=1}^{T} \frac{P_{t,s}^{d,b}}{\eta_d}, \tag{4.10}$$

$$\underline{P} \leq (P_{t,s}^{in,PL} - P_{t,s}^{out,PL}) + \sum_{b=1}^{N_{bess}} (P_{t,s}^{c,b} - P_{t,s}^{d,b}) \leq \overline{P}. \tag{4.11}$$

According to battery charger specifications, Equations (4.5) and (4.6) impose the bounds on charging and discharging power. These two constraints also prohibit the simultaneous charging and discharging of a battery. Binary variable $\nu_{t,s}$ indicates the

charging/discharging status of the battery, 1 indicates charging whereas 0 indicates discharging. The SoC at time t, $SoC_{t,s}$ of a PHEV or a D-BESS depends on SoC at time $(t-1)$ and charging/discharging of battery during $(t-1)$ and t. This relation can be defined as Equation (4.7). The battery SoC is subjected to maximum and minimum limits as shown in Equation (4.8). The constraint (4.9) ensures the maximum possible SoC at the time of departure of PHEV. This constraint is related to PHEV owner satisfaction, and SoC^{max} can be replaced with PHEV owner's desired SoC level. The constraint (4.10) ensures that the D-BESSs' net storage used is equal to zero over a day. This constraint is required for next-day availability of D-BESS and continuity in scheduling. The net power demand/supply of PLs and D-BESSs is restricted to maximum and minimum limits by MGO as shown in Equation (4.11). This constraint requires coordination between D-BESSs aggregator and PL operator.

4.3.2 Microgrid cost function

The MGO schedules its assets and exchanges power with the other MGOs and DU to satisfy the consumers' (and prosumers') demands under its purview. The MGO aims to minimize the MTs' operating cost, power import cost, Spinning Reserves (SR) cost, and emission cost while maximizing the power export cost. Thus, the objective function for m^{th} MGO can be written as

$$f_{MG} = \sum_{s=1}^{N_s} \pi_s \sum_{t=1}^{T} (C_{t,s}^{MT} + P_{t,s}^{im,m}\rho_t^{im,m} - P_{t,s}^{ex,m}\rho_t^{ex,m} + C_{t,s}^{SR} + P_{t,s}^{MT}\rho^{emi}). \tag{4.12}$$

Here, import and export powers of MG are denoted by $P_{t,s}^{im,m}$ and $P_{t,s}^{ex,m}$, respectively. MTs' generation cost $C_{t,s}^{MT}$ and spinning reserves cost $C_{t,s}^{SR}$ can be defined as

$$C_{t,s}^{MT} = \beta^{MT} P_{t,s}^{MT} + \gamma^{MT} (P_{t,s}^{MT})^2, \tag{4.13}$$

$$C_{t,s}^{SR} = (S_{t,s}^{up,MT} + S_{t,s}^{up,b})\rho_t^{up} + (S_{t,s}^{do,MT} + S_{t,s}^{do,b})\rho_t^{do} + P_{t,s}^{cur}\rho_t^{cur}. \tag{4.14}$$

The cost function of MT, $C_{t,s}^{MT}$ can be linearized by using a piece-wise linear function [130]. The SR cost of MG includes the D-BESSs' and MTs' SR cost, and the expected RESs curtailment cost in case of insufficient down-SR.

The MGO problem is subjected to some constraints, i.e., MT operating limits, RESs power availability, power exchange bounds, consumers load elasticity limits, spinning

reserves requirement, and load balancing. These constraints can be described as follows.

$$P_{t,s}^{im,m} \leq \nu_{t,s}^{exc,m} P^{immax,m}, \tag{4.15}$$

$$P_{t,s}^{ex,m} \leq (1 - \nu_{t,s}^{exc,m}) P^{exmax,m}, \tag{4.16}$$

$$\nu_{t,s}^{MT} P^{MTmin} \leq P_{t,s}^{MT} \leq \overline{P_{t,s}^{MT}}, \tag{4.17}$$

$$0 \leq \overline{P_{t,s}^{MT}} \leq \nu_{t,s}^{MT} P^{MTmax}, \tag{4.18}$$

$$\overline{P_{t,s}^{MT}} - P_{t-1,s}^{MT} \leq \nu_{t-1,s}^{MT} RU^{MT} + (\nu_{t,s}^{MT} - \nu_{t-1,s}^{MT}) SU^{MT} + (1 - \nu_{t,s}^{MT}) P^{MTmax}, \tag{4.19}$$

$$P_{t-1,s}^{MT} - P_{t,s}^{MT} \leq \nu_{t,s}^{MT} RD^{MT} + (\nu_{t-1,s}^{MT} - \nu_{t,s}^{MT}) SD^{MT} + (1 - \nu_{t-1,s}^{MT}) P^{MTmax}, \tag{4.20}$$

$$\overline{P_{t,s}^{MT}} \leq \nu_{t+1,s}^{MT} P^{MTmax} + (\nu_{t,s}^{MT} - \nu_{t+1,s}^{MT}) SU^{MT}, \tag{4.21}$$

$$P_{t,s}^{SL} = P_{t,s}^{L} \left[1 + \sum_{t'=1}^{T} E_{t,t'} \left(\frac{\rho_{t',s}^{new} - \rho_{t'}}{\rho_{t'}} \right) \right], \tag{4.22}$$

$$\underline{\Delta P} \leq (P_{t,s}^{SL} - P_{t,s}^{L}) \leq \overline{\Delta P}, \tag{4.23}$$

$$\sum_{t=1}^{T} (P_{t,s}^{SL} - P_{t,s}^{L}) = 0, \tag{4.24}$$

$$P_{t,s}^{im,m} + P_{t,s}^{MT} + P_{t,s}^{W} + P_{t,s}^{PV} - P_{t,s}^{ex,m} - P_{t,s}^{SL} - P_{t,s}^{in,PL} + P_{t,s}^{out,PL} - \sum_{b=1}^{N_{bess}} (P_{t,s}^{c,b} - P_{t,s}^{d,b}) = 0, \tag{4.25}$$

$$S_{t,s}^{up,MT} \leq min((\overline{P_{t,s}^{MT}} - P_{t,s}^{MT}), \nu_{t,s}^{MT} RU^{MT}), \tag{4.26}$$

$$S_{t,s}^{do,MT} \leq min((P_{t,s}^{MT} - \nu_{t,s}^{MT} P^{MTmin}), \nu_{t,s}^{MT} RD^{MT}), \tag{4.27}$$

$$S_{t,s}^{up,b} \leq min((P^{dmax} - P_{t,s}^{d,b} + P_{t,s}^{c,b}), (0.01 \eta_d BC(SoC_{t,s}^{b} - SoC^{min}))), \tag{4.28}$$

$$S_{t,s}^{do,b} \leq min((P^{cmax} - P_{t,s}^{c,b} + P_{t,s}^{d,b}), (\frac{0.01BC}{\eta_c}(SoC^{max} - SoC_{t,s}^{b}))), \tag{4.29}$$

$$P_{t,s}^{W} - P_{t}^{Wmin} + P_{t,s}^{PV} - P_{t}^{PVmin} - (S_{t,s}^{up,MT} + \sum_{b=1}^{N_{bess}} S_{t,s}^{up,b}) \leq 0, \tag{4.30}$$

$$P_{t}^{Wmax} - P_{t,s}^{W} + P_{t}^{PVmax} - P_{t,s}^{PV} - (S_{t,s}^{do,MT} + \sum_{b=1}^{N_{bess}} S_{t,s}^{do,b}) - P_{t,s}^{cur} \leq 0. \tag{4.31}$$

The maximum power import/export limits are bounded by constraints (4.15) and (4.16). Also, these two constraints prohibit simultaneous power import and export by the m^{th} MGO. Binary variable $u_{t,s}^{exc,m}$ represents the import/export status of MG, 1 indicates import whereas 0 indicates export of power. Constraints (4.17) and (4.18) limit the MT power generation $P_{t,s}^{MT}$. Ramp-up and ramp-down limits are imposed by Equations (4.19)-

(4.21) [130]. RU^{MT}/RD^{MT} are the ramp-up/down limits, whereas SU^{MT}/SD^{MT} are the startup/shutdown ramp limits of MT. Time-of-Use (TOU) based Demand Response (DR) is modeled by using the price elasticity of demand [131]. The elastic load represented by $P^{L}_{t,s}$ and $P^{SL}_{t,s}$, respectively indicating the demand before and after shifting the load. A linear response function of price elasticity (4.22) is used to obtain the modified demand. Equation (4.23) bounds the load shift in the DR program to an allowable limit. Constraint (4.24) indicates that there is no load curtailment in the DR program, i.e., consumer load can be shifted from one time period to another time period. Load balancing constraint (4.25) is a coupling constraint for MG, PLs, and D-BESSs.

The up-SR availability of MT (4.26) is subjected to scheduled output power, $P^{MT}_{t,s}$ and maximum available capacity, $\overline{P^{MT}_{t,s}}$ at that time. It must also satisfy the ramp-up limit of the generator. Similarly, the down-SR capability (4.27) depends on the ramp-down limit, and the difference between $P^{MT}_{t,s}$ and the lower limit of MT. The D-BESS contribution in SR depends on present SoC, charging/discharging state, and maximum limits of charging/discharging power. The up-SR (or down-SR) of D-BESS can be defined as maximum effective power injection (or absorbing) capability of D-BESS into (or from) the MG at that instant. The up- and down-SR are calculated using (4.28) and (4.29), respectively. The minimum up/down-SR requirement for reliable operation to manage the uncertainty of RESs can be defined by (4.30) and (4.31). In this work, we consider that the up-SR should be greater than the difference between total energy harvested from RESs ($P^{W}_{t,s} + P^{PV}_{t,s}$) and minimum expected RESs power ($P^{Wmin}_{t} + P^{PVmin}_{t}$) in all scenarios in that interval. The down-SR should be greater than the difference between the maximum expected RESs power ($P^{Wmax}_{t} + P^{PVmax}_{t}$) and total energy harvested from RESs.

4.4 Methodology

4.4.1 Decentralized scheduling based on Stochastic Dantzig-Wolfe decomposition

The PL operator, D-BESS aggregator, and MGO need a coordinated operation to satisfy coupling constraints. But they may be concerned about their privacy and want to share the minimum possible information for coordination. A decentralized technique is re-

quired to tackle this optimization problem. A decentralized approach, the Dantzig-Wolfe Decomposition Method (DWDM) [119], can be used to find the optimal global solution of a linear optimization problem with some coupling constraints. The problem described in section 4.3 can be optimized in a decentralized manner by using Stochastic Dantzig-Wolfe Decomposition (SDWD). The constraints (4.11), (4.25), (4.30), and (4.31) are coupling constraints, as these four constraints contain variables related to two or more operators, i.e. PL operator, D-BESS aggregator, and MGO. The original optimization problem can be restructured as two sub-problems (related to PL operator and D-BESS aggregator) and one master problem. All coupling constraints and MGO related constraints are associated with the master problem. The dual variables from the master-problem are used to penalize the sub-problems. So, the PL operator and D-BESS aggregator manage their scheduling according to these dual variables and energy tariff provided by MGO. They only need to share their net electricity demand proposals with MGO rather than personal data of individual consumers like arrival time, departure time, and battery energy level etc. The detailed mathematical reformulation can be described as Master-problem and Sub-problems in the following manner.

The Master-problem

$$min \sum_{s=1}^{N_s} \pi_s \sum_{t=1}^{T} \Bigg[(C_{t,s}^{MT} + P_{t,s}^{im,m} \rho_t^{im,m} - P_{t,s}^{ex,m} \rho_t^{ex,m} + S_{t,s}^{up,MT} \rho_t^{up} + S_{t,s}^{do,MT} \rho_t^{do} + P_{t,s}^{cur} \rho_t^{cur} + P_{t,s}^{MT} \rho^{emi}) + \sum_{\omega} (Z_{\omega,s}^{PL} u_{\omega}^{PL} + Z_{\omega,s}^{BESS} u_{\omega}^{BESS}) \Bigg] + \sum_{t=1}^{T} pen_t. \quad (4.32)$$

Here, $Z_{\omega,s}^{PL}$ and $Z_{\omega,s}^{BESS}$ are cost related to PL and D-BESS for ω^{th} proposal. The decision variables u_{ω}^{PL} and u_{ω}^{BESS} assign weights to the PL operator and D-BESS aggregator proposals. $Z_{\omega,s}^{PL}$ and $Z_{\omega,s}^{BESS}$ can be defined as

$$Z_{\omega,s}^{PL} = \sum_{t=1}^{T} (P_{\omega,t,s}^{in,PL} \rho_t^c - P_{\omega,t,s}^{out,PL} \rho_t^d), \quad (4.33)$$

$$Z_{\omega,s}^{BESS} = \sum_{t=1}^{T} \sum_{b=1}^{N_{bess}} (P_{\omega,t,s}^{c,b} \rho_t^c - P_{\omega,t,s}^{d,b} \rho_t^d + S_{\omega,t,s}^{do,b} \rho_t^{do} + S_{\omega,t,s}^{up,b} \rho_t^{up}). \quad (4.34)$$

A factor,$\sum_{t=1}^{T} pen_t$ is used to force the MGO to minimize the changes in hourly net power demand in two consecutive iterations. K increase linearly as the iteration count increases.

$$pen_t = K\left(\left|\sum_{s=1}^{N_s}\pi_s P_{t,s}^{im,m} - P_{t,iter-1}^{im,m}\right| + \left|\sum_{s=1}^{N_s}\pi_s P_{t,s}^{ex,m} - P_{t,iter-1}^{ex,m}\right|\right). \tag{4.35}$$

subject to

$$P_{t,s}^{im,m} + P_{t,s}^{MT} + P_{t,s}^{W} + P_{t,s}^{PV} - P_{t,s}^{ex,m} - P_{t,s}^{SL} - \sum_{\omega}(P_{\omega,t,s}^{in,PL} - P_{\omega,t,s}^{out,PL})u_{\omega}^{PL} - \sum_{\omega}\sum_{b=1}^{N_{bess}}(P_{\omega,t,s}^{c,b} - P_{\omega,t,s}^{d,b})u_{\omega}^{BESS} = 0 \qquad \boldsymbol{\lambda_{t,s}^{1}}, \tag{4.36}$$

$$\underline{P} \leq \sum_{\omega}(P_{\omega,t,s}^{in,PL} - P_{\omega,t,s}^{out,PL})u_{\omega}^{PL} - \sum_{\omega}\sum_{b=1}^{N_{bess}}(P_{\omega,t,s}^{c,b} - P_{\omega,t,s}^{d,b})u_{\omega}^{BESS} \leq \overline{P} \qquad \boldsymbol{\lambda_{t,s}^{2}, \lambda_{t,s}^{3}}, \tag{4.37}$$

$$P_{t}^{Wmax} - P_{t,s}^{W} - P_{t}^{PVmax} - P_{t,s}^{PV} - S_{t,s}^{do,MT} - P_{t,s}^{cur} - \sum_{\omega}\sum_{b=1}^{N_{bess}} S_{\omega,t,s}^{do,b}u_{\omega}^{BESS} \leq 0 \qquad \boldsymbol{\lambda_{t,s}^{4}}, \tag{4.38}$$

$$P_{t,s}^{W} - P_{t}^{Wmin} + P_{t,s}^{PV} - P_{t}^{PVmin} - S_{t,s}^{up,MT} - \sum_{\omega}\sum_{b=1}^{N_{bess}} S_{\omega,t,s}^{up,b}u_{\omega}^{BESS} \leq 0 \qquad \boldsymbol{\lambda_{t,s}^{5}}, \tag{4.39}$$

$$\sum_{\omega} u_{\omega}^{PL} = 1 \qquad \boldsymbol{\sigma_{PL}}, \tag{4.40}$$

$$\sum_{\omega} u_{\omega}^{BESS} = 1 \qquad \boldsymbol{\sigma_{BESS}}, \tag{4.41}$$

$$u_{\omega}^{PL}, u_{\omega}^{BESS} \geq 0, \tag{4.42}$$

in addition to constraints (4.15)-(4.24), (4.26), and (4.27).

The load balancing constraint (4.36), prosumers' demand limits (4.37), and spinning reserves (4.38)-(4.39) represent coupling constraints. Equations (4.40) and (4.41) are convexity constraints. $\lambda_{t,s}^{m}$, σ_{PL}, and σ_{BESS} indicate the dual variables.

The Sub-problems

The master problem proposes dual variables $\lambda_{t,s}^{m}$, σ_{PL}, and σ_{BESS} to the PL operators and D-BESS aggregators. Based on these dual variables, PL operators and D-BESS aggregators optimize their respective sub-problems to generate new proposals. The PL operators' and D-BESS aggregators' sub-problems are characterized by (4.43) and (4.44), respectively.

$$min \sum_{t=1}^{T}\sum_{s=1}^{N_s}\left(\left(\rho_t^c\pi_s + \sum_{m=1}^{3}\lambda_{t,s}^{m}\right)P_{t,s}^{in,PL} + \left(-\rho_t^d\pi_s - \sum_{m=1}^{3}\lambda_{t,s}^{m}\right)P_{t,s}^{out,PL}\right) - \sigma_{PL}, \tag{4.43}$$

subject to constraints (4.5)-(4.9).

$$min \sum_{t=1}^{T}\sum_{s=1}^{N_s}\sum_{b=1}^{N_{bess}}\Bigg(\Bigg(\rho_t^c\pi_s + \sum_{m=1}^{3}\lambda_{t,s}^m\Bigg)P_{t,s}^{c,b} + \Bigg(-\rho_t^d\pi_s - \sum_{m=1}^{3}\lambda_{t,s}^m\Bigg)P_{t,s}^{d,b} + \Bigg(\rho_t^{do}\pi_s + \lambda_{t,s}^4\Bigg)S_{t,s}^{do,b} + \Bigg(\rho_t^{up}\pi_s + \lambda_{t,s}^5\Bigg)S_{t,s}^{up,b}\Bigg) - \sigma_{BESS}, \quad (4.44)$$

subject to constraints (4.5)-(4.8), (4.10), (4.28) and (4.29).

4.4.2 Shapley value method for cost/profit allocation

In cooperative game theory, the SVM is a concept to fairly allocate profit/cost to all the players working in a coalition. The SVM also effectively considers the unequal contribution of each player working in a coalition. Let, the total number of MGs be n, and $|S|$ be the total number of MGs in coalition S, where $|S| \leq n$. The Shapley Value, ϕ_t^m for time period t for m^{th} MG, can be calculated as,

$$\phi_t^m = \sum_{S}\Bigg(\frac{(n- \mid S \mid)!(\mid S \mid -1)!}{n!}\Bigg)\Bigg(\psi_t(S) - \psi_t(S - \{m\})\Bigg). \quad (4.45)$$

Here, $\psi_t(S)$ is the total profit/cost of coalition S and $\psi_t(S - \{m\})$ is the profit/cost of coalition S without participation of m^{th} MG. The $\psi_t(S)$ can be defined as

$$\psi_t(S) = \sum_{m\in S}\Bigg(P_t^{im,m}\rho_t^{im,m} - P_t^{ex,m}\rho_t^{ex,m}\Bigg) - \Bigg(max\Bigg(0, \sum_{m\in S}\Bigg(P_t^{im,m} - P_t^{ex,m}\Bigg)\Bigg)\rho_t^{c,du} + min\Bigg(0, \sum_{m\in S}\Bigg(P_t^{im,m} - P_t^{ex,m}\Bigg)\Bigg)\rho_t^{d,du}\Bigg). \quad (4.46)$$

4.4.3 Tariff update

After fairly allocating the hourly profit/cost, the tariff for all the MGs can be updated for the next iteration in the following manner.

$$\rho_{t,iter+1}^{im,m} = \begin{cases} \frac{P_t^{im,m}\rho_t^{im,m} - \phi_t^m}{P_t^{im,m}}, & \text{if } P_t^{im,m} \neq 0 \\ \rho_t^{im,m}, & \text{otherwise,} \end{cases} \quad (4.47)$$

and

$$\rho_{t,iter+1}^{ex,m} = \begin{cases} \frac{P_t^{ex,m}\rho_t^{ex,m} + \phi_t^m}{P_t^{ex,m}}, & \text{if } P_t^{ex,m} \neq 0 \\ \rho_t^{ex,m}, & \text{otherwise.} \end{cases} \quad (4.48)$$

Based on the tariff updated by MGA for MGs, the MGO updates tariff of its prosumers and consumers. The updated tariff for prosumers and consumers can be written as,

$$\rho^{c}_{t,iter+1} = \begin{cases} 1.1\rho^{im,m}_{t,iter+1}, & \text{if } P^{im,m}_{t} \neq 0 \\ 1.1\rho^{ex,m}_{t,iter+1}, & \text{if } P^{ex,m}_{t} \neq 0 \\ \rho^{c}_{t}, & \text{otherwise,} \end{cases} \tag{4.49}$$

and

$$\rho^{d}_{t,iter+1} = \begin{cases} 0.9\rho^{im,m}_{t,iter+1}, & \text{if } P^{im,m}_{t} \neq 0 \\ 0.9\rho^{ex,m}_{t,iter+1}, & \text{if } P^{ex,m}_{t} \neq 0 \\ \rho^{d}_{t}, & \text{otherwise.} \end{cases} \tag{4.50}$$

4.4.4 Decentralized scheduling algorithm for network connected multi-microgrids system

The energy management framework[1] used in this study is depicted in Figure 4.4. In this framework, MGOs perform a decentralized energy management optimization parallelly to meet consumer demand after collecting data at the first level. The Stochastic Dantzig-Wolfe Decomposition (SDWD) method is used for decentralized energy management optimization. SDWD converges to the optimal point by iterating between the master problem and the sub-problems of PLs and D-BESSs. The master-problem contains the MG's constraints (4.15)-(4.24), (4.26), (4.27) and all the coupling constraints (4.36)-(4.39). MGO solves the master problem (4.32) and calculate the optimal dual variables associated with coupling constraints (4.36)-(4.39) and convexity constraints (4.40)-(4.41). The values of dual variables are then communicated to the PL operator and D-BESS aggregator sub-problems. The PL operator and D-BESS aggregator use these dual variables to solve their respective sub-problems and propose the new proposals to the master problem. This process of exchanging dual variables and proposals continues until the convergence of SDWD. Followed by this optimization, all MGOs send their energy requests to MGA. After that, MGA updates tariffs according to MGOs' power exchange requests

[1]The approximate bandwidth required to meet the communication requirement of the proposed method with a single PL operator and D-BESS aggregator is approximately 4 Mbps (up-link) and 2 Mbps (down-link) for 20 ms latency. Existing 4G communication technologies are sufficient to meet the communication requirement for the proposed algorithm.

as given in (4.47)-(4.48). For rescheduling, the MGOs determine the tariffs (4.49)-(4.50) for their prosumers and consumers after receiving new tariffs from the MGA. This process is repeated until the stopping criterion is reached.

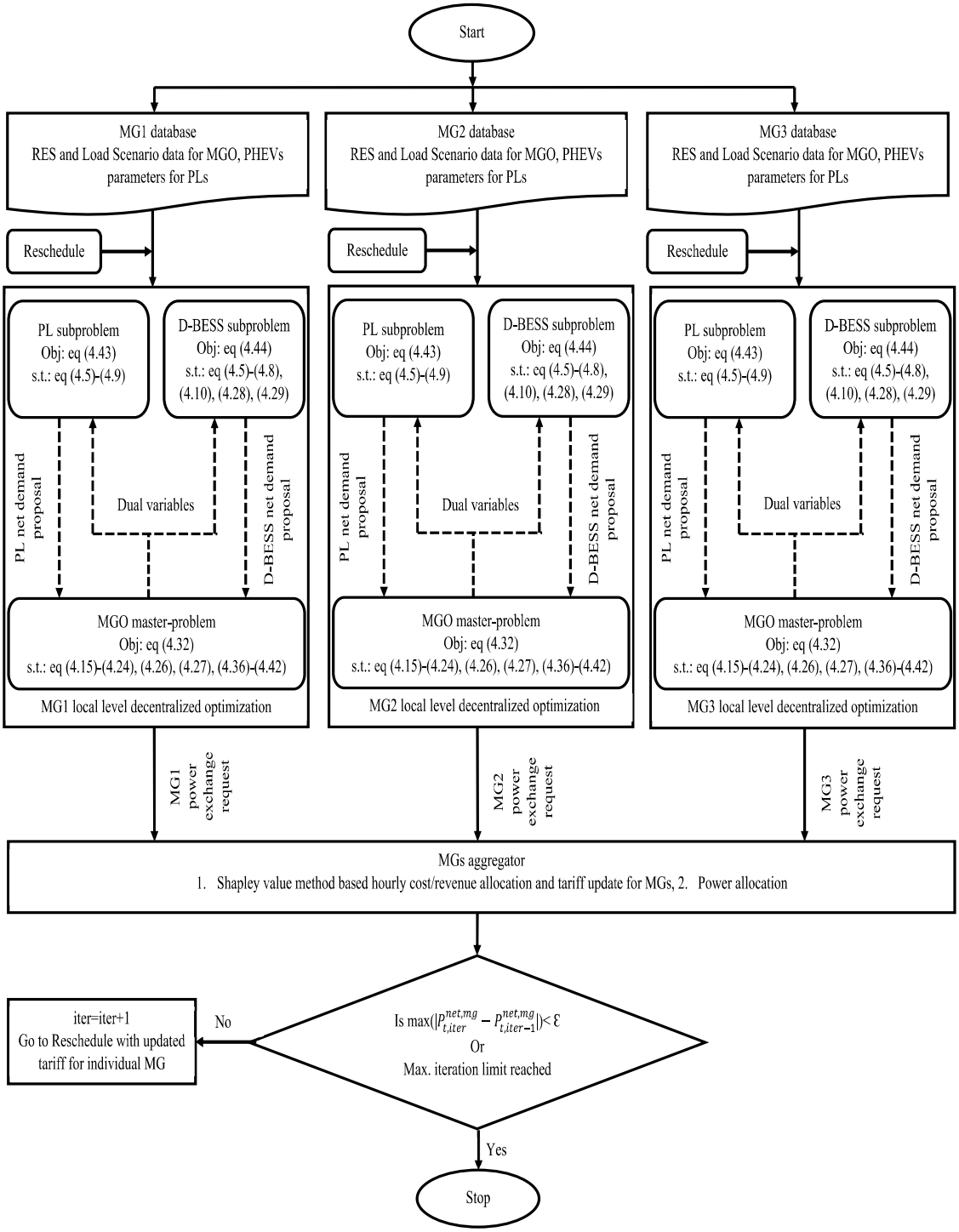

Figure 4.4: Energy management framework flow diagram

Reformulation of the original problem into master problem and sub-problems in the Dantzig-Wolfe Decomposition Method (DWDM) framework does not change the optimal solution of original problem. The solution path of the master problem with a more complex feasible region may be longer than the original problem. In actual practice, a compromise needs to be made between the accuracy of the optimal solution and the computation time.

4.5 Simulation results and discussions

4.5.1 System data

In this study, three MGs with different load profiles and generation capacities are considered. The predicted conventional elastic loads of MGs are depicted in Figure 4.5. The

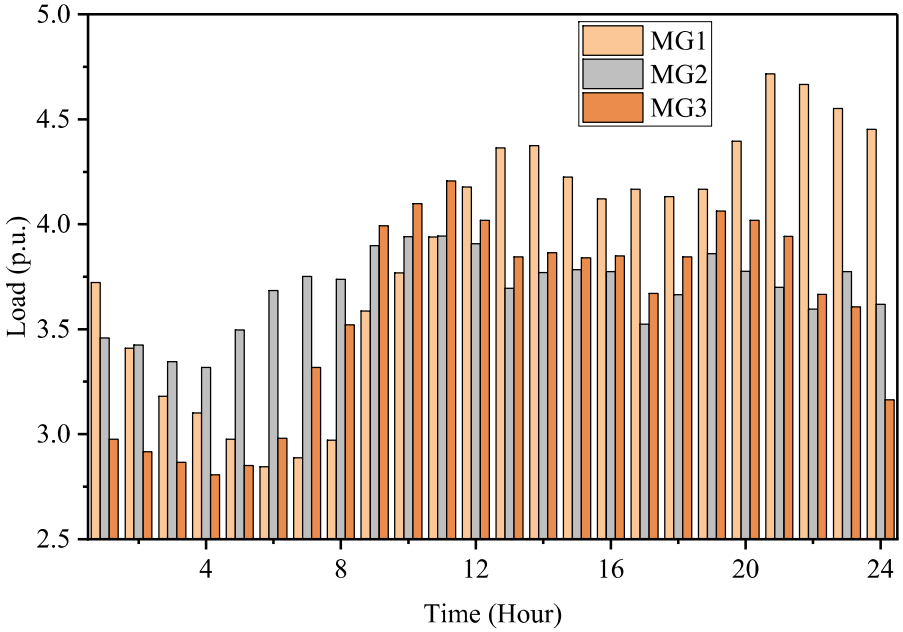

Figure 4.5: Load profile of MGs

assumed load elasticity coefficients are given in Table 4.1. The wind power ratings are 3 MW each for MG1 and MG3, and 3.5 MW for MG2. The PV rating is 1.5 MW for all the MGs. The rated capacities of MTs are 1.8 MW for MG1 and 1.5 MW for MG2 and MG3. The rated battery capacities are assumed to be 80 kW for D-BESSs and 15.6–27.6 kW for PHEVs [132]. The maximum charging and discharging rates are 40 kW/h for D-BESS. The charging and discharging efficiencies are assumed to be 95% [85]. The DU's

Table 4.1: Elasticity coefficients

	Peak Period	Shoulder Period	Valley Period
Peak Period	-0.2	0.016	0.012
Shoulder Period	0.008	-0.2	0.01
Valley Period	0.006	0.008	-0.2

Table 4.2: Distribution Utility's electricity tariff

Hours	1	2	3	4	5	6	7	8	9	10	11	12
$\rho_t^{c,du}$,€/kWh	0.071	0.063	0.058	0.053	0.054	0.061	0.071	0.085	0.087	0.095	0.105	0.113
Hours	13	14	15	16	17	18	19	20	21	22	23	24
$\rho_t^{c,du}$,€/kWh	0.112	0.120	0.132	0.144	0.150	0.146	0.142	0.126	0.129	0.127	0.114	0.093

day-ahead electricity tariff is given in Table 4.2. The feed-in tariff is considered as half of the electricity tariff. The emission rate is assumed to be 0.01695 €/kWh. The proposed framework has been implemented on a system with a Core i3, 1.20 GHz processor and 4 GB RAM. The GAMS/CPLEX solver is used for solving the optimization problems.

4.5.2 A comparative analysis of different power trading and pricing mechanisms

The following three cases are considered to demonstrate the effectiveness of the proposed EMS.

Case I (Base case): In this case, each MG optimizes its objective function, and there is no cooperation among MGs. All MGs exchange power with DU only.

Case II: In this case, the MGA acts as an intermediary among MGs and DU. The MGA receives power exchange requests from all MGs. Based on the power exchange requests, MGA allocates power among MGs and updates tariffs for MGs according to Shapley values.

In *Case I* and *Cases II*, each MG uses the updated tariff given in (4.49) and (4.50) for its prosumers and consumers.

Case III: This case is used for comparative analysis of proposed EMS with the existing state-of-art [105]. In this case, the tariff for MGs' prosumers and consumers is

based on DU's electricity tariff rather than the updated price given in (4.49) and (4.50). The ρ_t^c and ρ_t^d are assumed to be $1.1\rho_t^{c,du}$ and $0.9\rho_t^{d,du}$, respectively. In this case, following three sub-cases can be envisaged.

Case III(a): There is no power trading among MGs.

Case III(b): In this case the tariff updates for MGs' prosumers and consumers are not considered as per (4.49) and (4.50) and otherwise this case is similar to $Case\ II$.

Case III(c): In this case, the Nash bargaining theory-based incentive mechanism [105] is used for scheduling.

The power exchange requests of MGs are depicted in Figure 4.6(a) and 4.6(b) for $Case\ I$ and $Case\ II$, respectively. It can be seen that the MGs' scheduled power exchange increases in $Case\ II$ as compared to $Case\ I$, i.e., MG3 requests for more power import during 11:00 to 13:00 hours and during the same time interval, MG1 and MG2 increase their power export. The reason behind this change is the updated tariff for MGs due to cooperative scheduling and Shapley value allocation. The tariffs for MGs are represented in Figure 4.7(a) and 4.7(b) for $Case\ I$ and $Case\ II$, respectively. The dotted line in Figure 4.7 indicates the DU's energy tariff, while the solid line represents the DU's feed-in tariff. Figure 4.7(a) for $Case\ I$ depicts that the tariff corresponding to a particular MG is always equal to DU's energy selling (feed-in) price when the MG imports (exports) power, irrespective of power exchange scenarios of the other MGs. In $Case\ II$ (Figure 4.7(b)), the tariff for MG also depends on other MGs' circumstances. If some MGs in a coalition are willing to import the power and others consent to export power, they can settled on a price between DU's selling price and feed-in tariff. For example, in $Case\ II$, Figure 4.7(b), during 9:00 to 15:00, 18:00 to 20:00, and 22:00 to 24:00 hours, the energy prices are below DU's selling price but higher than the DU's feed-in tariff. This situation is advantageous for all participants in the coalition as they can reduce their power import price or increase their power export price. Therefore, the proposed pricing mechanism ensures that the energy import price for buyer MGs is always less than or equal to DU's energy tariff. The energy export price for seller MGs is always greater than or equal to DU's feed-in tariff. The tariff for an MG depends on two factors; the contribution of MG in the energy pool as a seller (buyer) and the deficit (surplus) amount of energy of other MGs. As shown in the Figure 4.7, the MG1 and MG2 are able to sell their power at a higher rate in $Case\ II$ compared to DU's feed-in tariff in $Case\ I$. Similarly, MG3 can

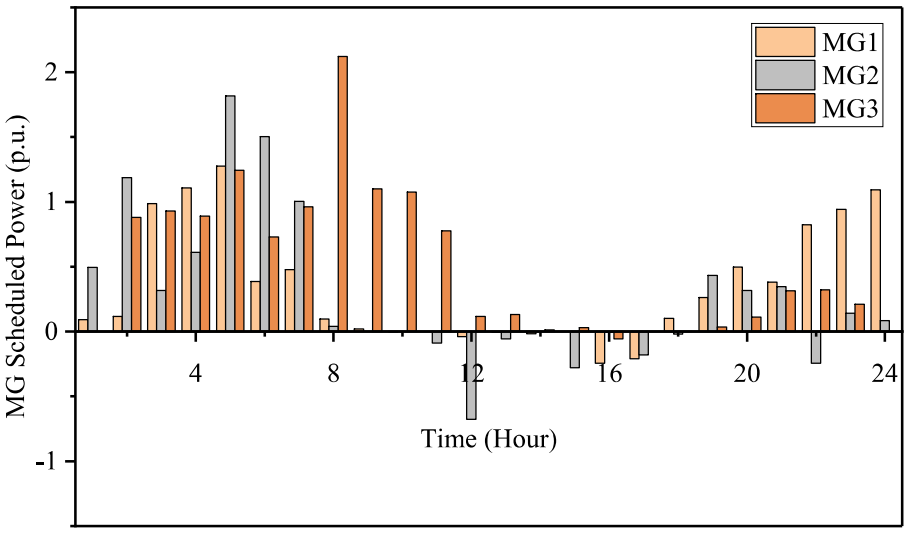

(a)

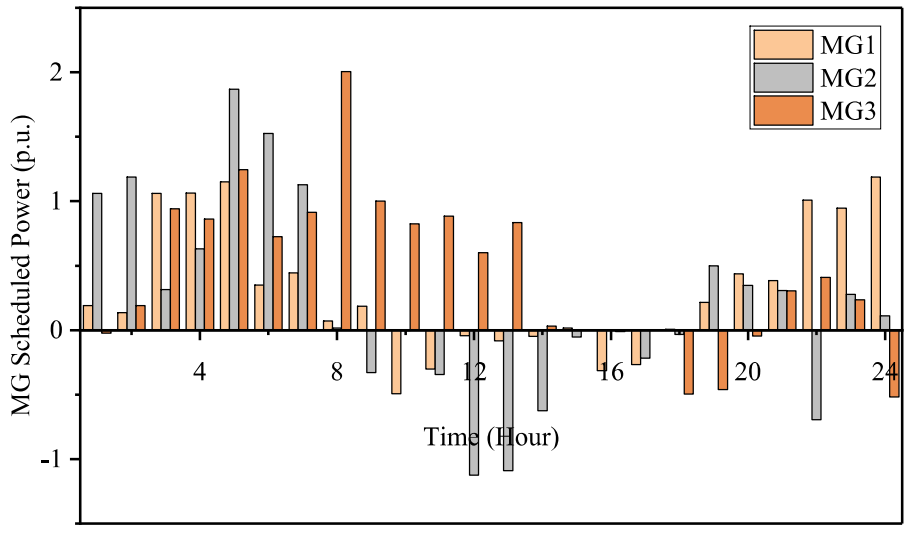

(b)

Figure 4.6: Scheduled power exchange of MGs (a) *Case I*, (b) *Case II*

purchase power at a lower rate as compared to DU's energy tariff at the same instant.

According to its power import (export) tariff, the MGO updates its charging (discharging) tariff for prosumers and consumers of its purview. Thus, as shown in Figures 4.8 and 4.9, the scheduled power demands of PLs and D-BESSs are also changed according to

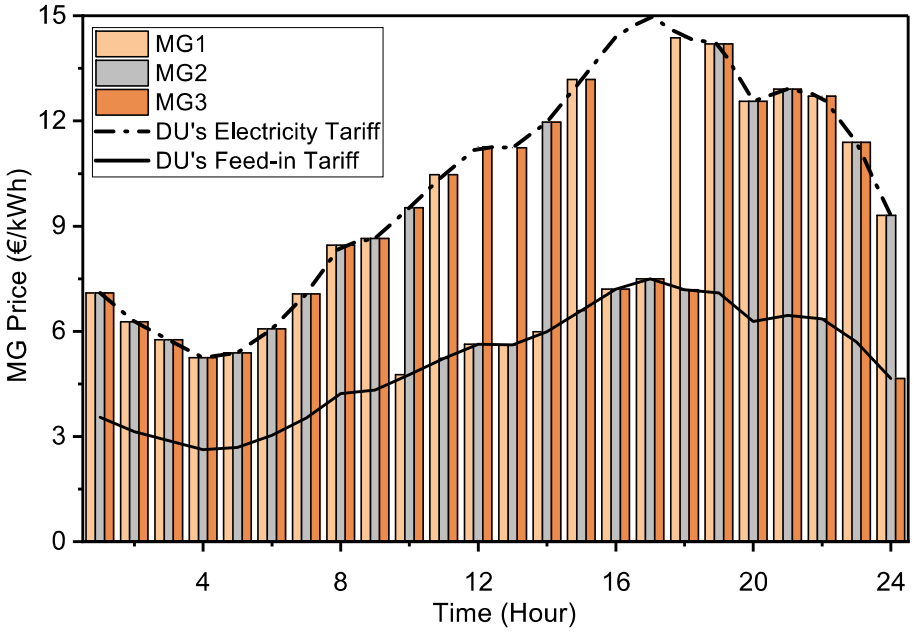

(a)

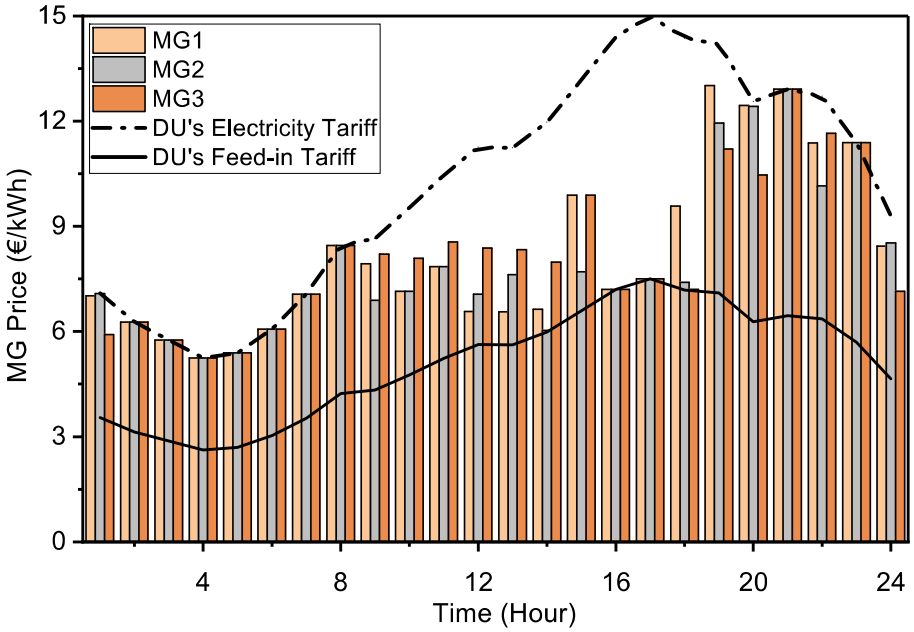

(b)

Figure 4.7: Power exchange tariff for MGs (a) *Case I*, (b) *Case II*

the tariff received by MGO. The power demand of PL in MG1 has a peak point at 10:00 hours in *Case I* because of the low tariff at this time interval compared to neighboring time intervals. But in *Case II*, the PL demand is distributed between 9:00 to 11:00 hours, as the tariff of MG1 increases at 10:00 hours and decreases at 9:00 and 11:00 hours. A similar pattern is observed for all the PLs and D-BESSs in *Case II*.

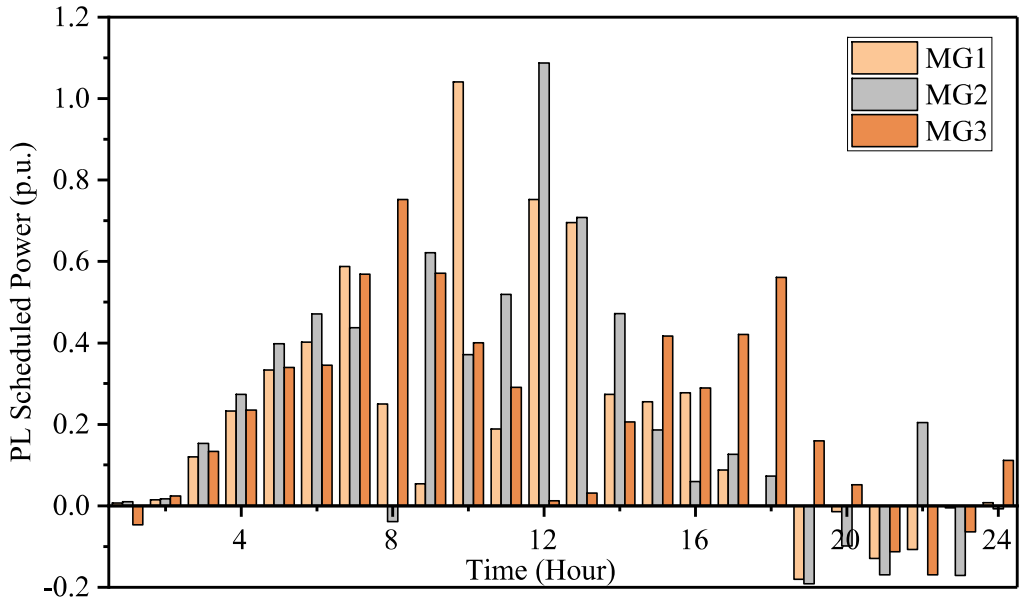

(a)

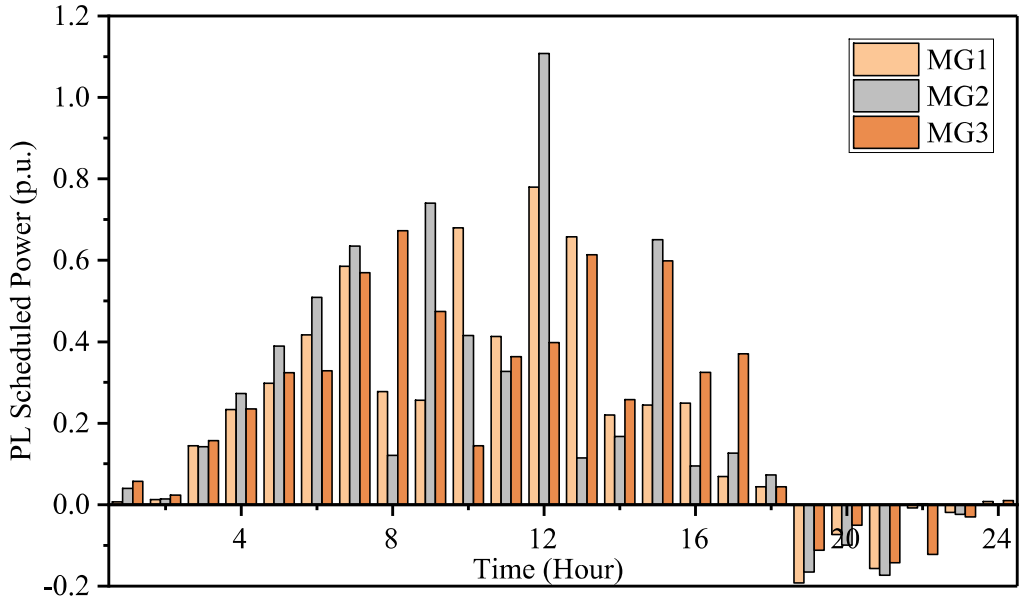

(b)

Figure 4.8: Scheduled power of PLs (a) *Case I*, (b) *Case II*

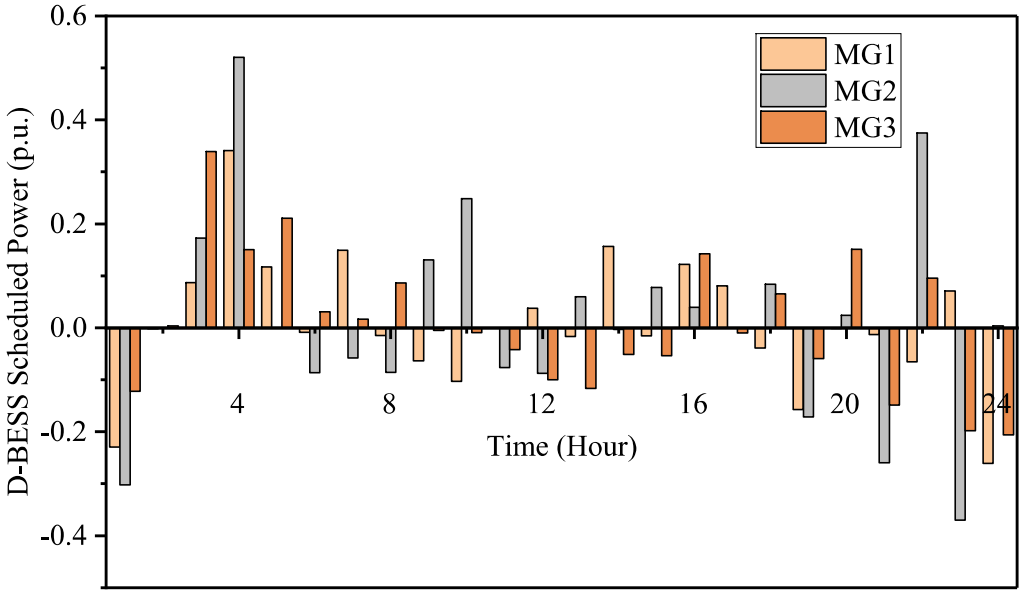

(a)

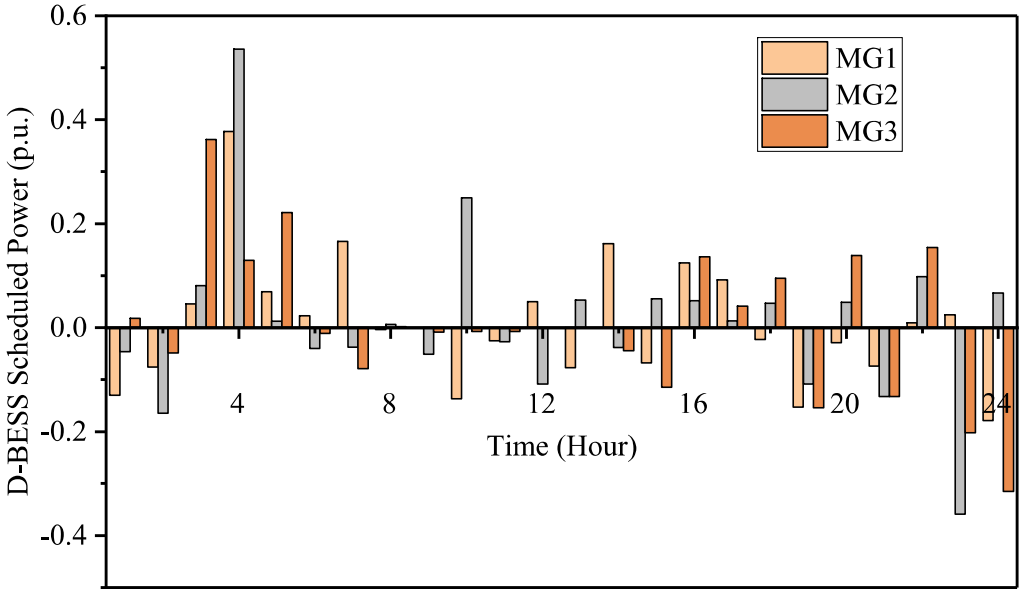

(b)

Figure 4.9: Scheduled power of D-BESS (a) *Case I*, (b) *Case II*

The power outputs of scheduled MTs are shown in Figure 4.10. The higher power export tariff encourages more power generation from MTs. MG1 and MG2 increase their generation during the mid-day period, when they export power, whereas MG3 imports power during the same duration. MG3 raises its generation at 24:00 hours to export power to MG1 and MG2. Besides the power export tariff, MT generation depends on its

ramp-rate constraints and other system conditions. There is no change in tariff in both the cases and there is a negligible difference between MG3 tariff and MT generation cost at 2:00 hours, so MT in MG3 generates more power to satisfy the demand and ramp-rate constraints.

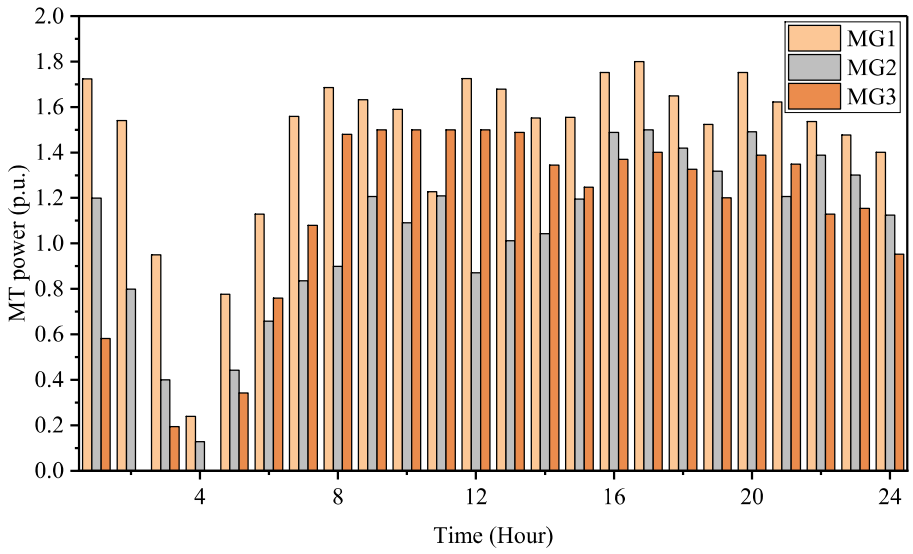

(a)

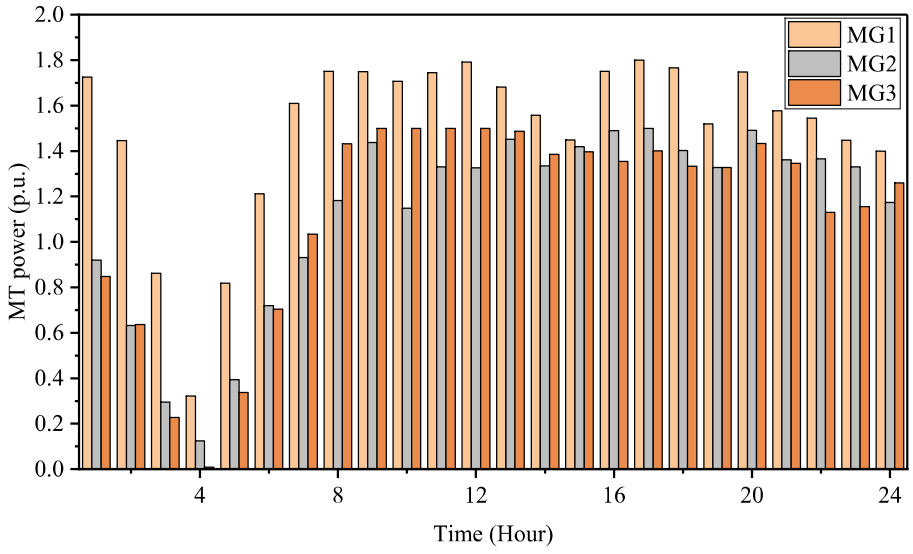

(b)

Figure 4.10: MT scheduled power (a) *Case I*, (b) *Case II*

The contributions of D-BESSs and MT in SR (up/down) to cope with the uncertainties due to RESs are shown in Figure 4.11. In both the cases, the spinning reserve

requirements are approximately the same. But the contributions of D-BESS and MT are different, as the scheduled powers are subjected to energy tariff. The expected RESs power curtailment to contribute in down-SR is shown in Figure 4.12. If MT and D-BESS are not

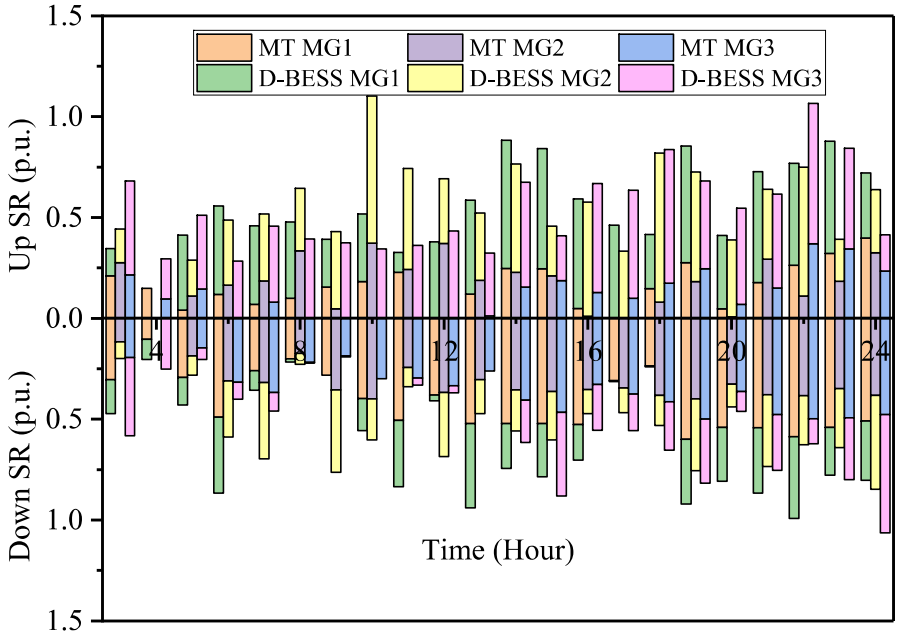

(a)

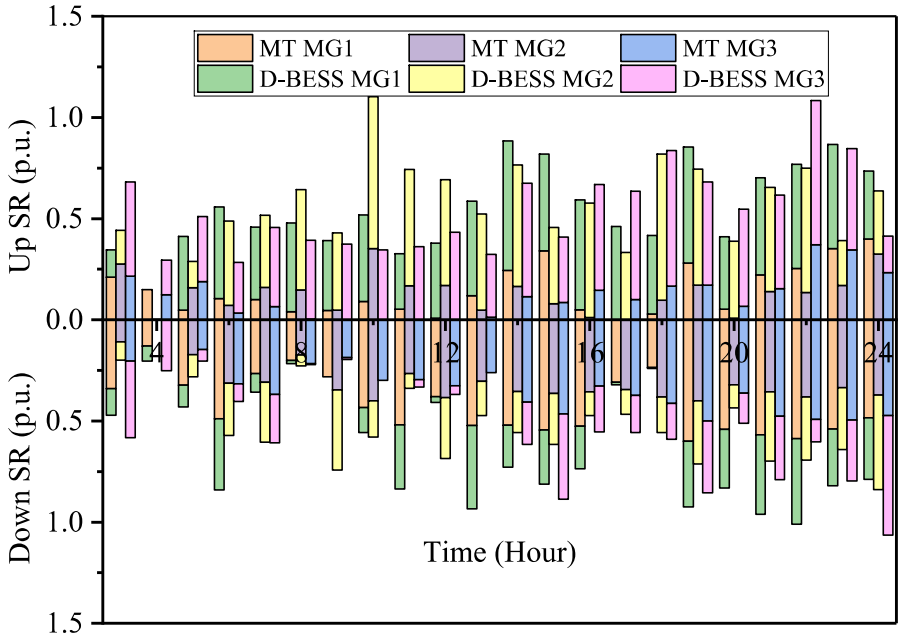

(b)

Figure 4.11: D-BESS and MT contribution in spinning reserves (a) *Case I*, (b) *Case II*

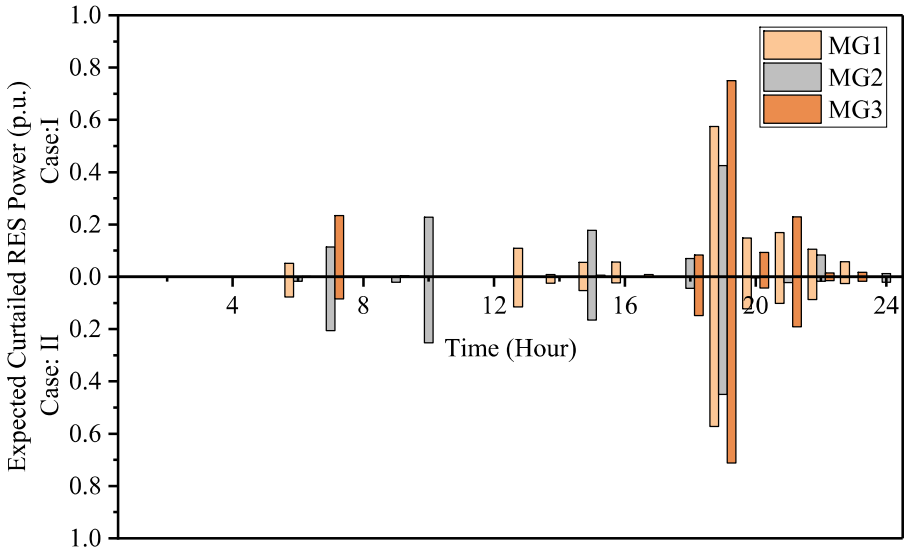

Figure 4.12: Expected RESs power curtailment

sufficient to fulfill the down-SR, RESs power is curtailed with high curtailment charges. The outcomes of both the cases are summarized in Table 4.3. In *Case II* the operation cost, which includes MT generation cost, power exchange cost, and SR cost, reduces from 3640.618 to 3584.588 €/day for MG1, 2905.860 to 2835.171 €/day for MG2, and 3398.049 to 3319.453 €/day for MG3. However, the cost of PLs increases from 343.633 to 379.376 €/day in MG1 and 368.925 to 399.365 €/day in MG2, while it reduces from 507.545 to 460.172 €/day in MG3. As stated above, MGOs provide tariffs to their prosumers and consumers based on the tariffs they receive from MGA. The PLs and D-BESSs optimize their storage schedule according to these tariffs. As seen in Figure 4.7, the MG1 and MG2 get higher tariffs when they export power during 8:00 to 14:00 hours in *Case II* compared to *Case I*. Most of the charging in PLs occurs during these hours due to the restriction of PHEVs' parking time slots, as shown in Figure 4.3(a). So, the PL operators in MG1 and MG2 have to pay higher amount for energy purchase in *Case II*. But MG3 imports energy during this duration at a lower rate as compared to *Case I*. So, the PL cost in MG3 reduces in *Case II*. The D-BESS aggregator profit increases in *Case II* as depicted in Table 4.3. D-BESSs have greater flexibility to shift their scheduling than PLs because they are not constrained by arrival and departure times. The overall energy cost, F, reduces from 3997.206 to 3976.016 €/day, 3280.124 to 3251.381 €/day, and 3917.076 to 3793.984 €/day for MG1, MG2, and MG3, respectively. The average power import

price for all the three MGs decreases by 5.368%, 2.844%, and 13.07%, while the average power export price for all MGs increases by 15.51%, 13.12%, and 13.85% in *Case II* as compared to *Case I*.

Table 4.3: Cost comparison for different cases

		Case I	*Case II*
MG operating Cost (€)	MG1	3640.618	3584.588
	MG2	2905.860	2835.171
	MG3	3398.049	3319.453
PLs' Cost (€)	MG1	343.633	379.376
	MG2	368.925	399.365
	MG3	507.545	460.172
D-BESSs' Cost (€)	MG1	-376.103	-386.845
	MG2	-389.785	-407.258
	MG3	-380.731	-388.249
F (€)	MG1	3997.206	3976.016
	MG2	3280.124	3251.381
	MG3	3917.076	3793.984
Avg power import price (€/kWh)	MG1	0.092	0.087
	MG2	0.086	0.083
	MG3	0.094	0.082
Avg power export price (€/kWh)	MG1	0.061	0.071
	MG2	0.067	0.075
	MG3	0.071	0.082

The net demand of all the three MGs for *Case III* is shown in Figure 4.13. MGs exchange more power in *Case III*(b) and *Case III*(c) as compared to *Case III*(a). However, both mechanisms used in *Case III*(b) and *Case III*(c) encourage MGs to trade power among themselves. But the net demands of MGs are not exactly the same in *Case III*(b) and *Case III*(c). The allocation of SVM-based hourly profit/cost is used

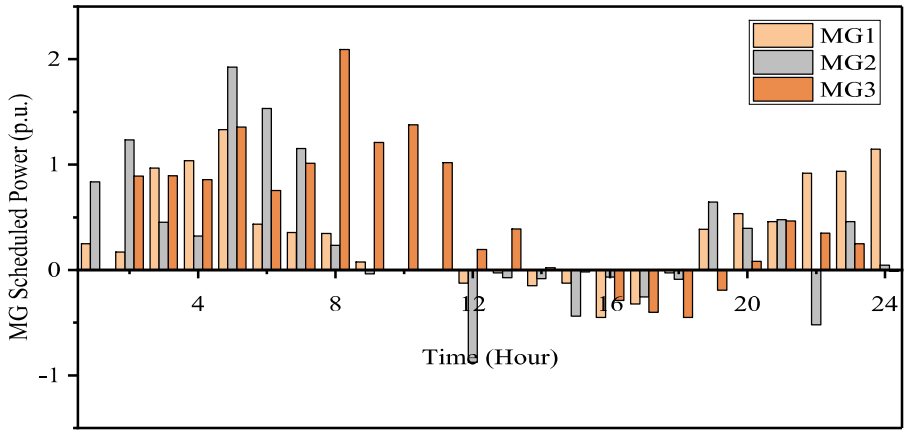

(a)

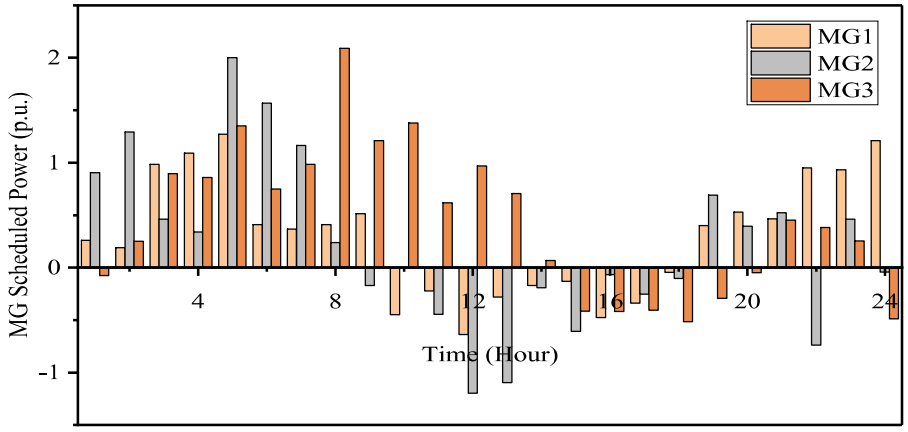

(b)

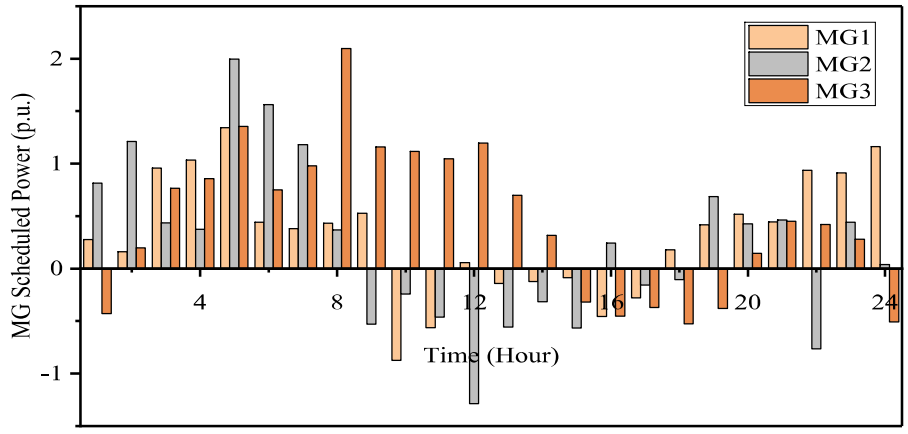

(c)

Figure 4.13: MGs' scheduled power (a) *Case III*(a), (b) *Case III*(b), (c) *Case III*(c)

to update MGs' import/export tariffs in *Case III*(*b*). Whereas, the Nash bargaining method in *Case III*(*c*) is used to distribute the profit among MGs after the cooperative scheduling to reduce the energy cost functions, F, of all MGs. The cost comparison of *Case III* is depicted in Table 4.4. The MG operating cost is lower in *Case III*(*b*) as

Table 4.4: Cost comparison for *Case III*

		Case III(*a*)	*Case III*(*b*)	*Case III*(*c*)
MG operating	MG1	3680.374	3651.316	3665.588
	MG2	2974.824	2928.177	2959.833
Cost (€)	MG3	3444.901	3378.979	3430.107
PLs'	MG1	514.308	504.745	499.521
	MG2	532.233	528.48	517.242
Cost (€)	MG3	563.601	551.722	548.808
D-BESSs'	MG1	-374.191	-384.372	-388.977
	MG2	-397.859	-407.354	-412.851
Cost (€)	MG3	-359.793	-369.949	-374.587
F (€)	MG1	4229.259	4186.263	4171.888
	MG2	3532.070	3473.867	3474.699
	MG3	4051.723	3958.735	3994.354

compared to *Case III*(*a*) and *Case III*(*c*). The total energy cost of all MGs, i.e., the sum of energy cost functions, F, of all MGs, are 11813.052, 11618.865 and 11640.941 €/day for *Case III*(*a*), *Case III*(*b*) and *Case III*(*c*), respectively. So, the total energy cost of all MGs is almost same for *Case III*(*b*) and *Case III*(*c*) as compared to *Case III*(*a*). Also, *Case III*(*b*) appears marginally better than *Case III*(*c*), and the energy cost functions, F, of all MGs are much lower in *Case II* as compared to *Case III*. Therefore, the proposed EMS can effectively reduce energy costs.

4.6 Summary

The numerical results establish the effectiveness of the proposed energy management approach to minimize the energy cost. A Dantzig-Wolfe Decomposition (DWD) is an efficient tool for achieving the goals of MGO, PL operators and D-BESS aggregators in a decentralized fashion with minimal information exchange. The D-BESSs and MTs can be used as spinning reserves to cope with the associated uncertainties in the system. The MG aggregator uses the Shapley Value Method (SVM) to fairly allocate the cost/revenue and update the energy tariff for MGO. The results show that hourly power import price of each MGO is less than or equal to the tariff of distribution utility (DU) and hourly power export price of each MGO is higher than or equal to feed-in tariff of DU. This updated energy tariff at MG aggregator level prompts MGOs to exchange power among themselves rather than with DU. The cost comparison demonstrates that cooperative operation in the proposed framework yields significant reduction in the MGs' operating cost. Also, the average power import price significantly decreases while the average power export price increases in a cooperative approach. Thus, the proposed technique is beneficial in terms of cost savings as well as less dependence on distribution utility.